ResearchGate

See discussions, stats, and author profiles for this publication at: https://www.researchgate.net/publication/220018981

Flexible sensorial system based on capacitive chemical sensors integrated with readout circuits fully fabricated on ultra thin substrate

ARTICLE *in* SENSORS AND ACTUATORS B CHEMICAL · JULY 2011

Impact Factor: 4.1 · DOI: 10.1016/j.snb.2011.01.045

CITATIONS
20

READS
73

11 AUTHORS, INCLUDING:

Luca Maiolo
Italian National Research Council
74 PUBLICATIONS **301** CITATIONS
SEE PROFILE

Alessandro Pecora
Italian National Research Council
134 PUBLICATIONS **941** CITATIONS
SEE PROFILE

Antonella Macagnano
Italian National Research Council
137 PUBLICATIONS **2,275** CITATIONS
SEE PROFILE

Andrea Bearzotti
Italian National Research Council
101 PUBLICATIONS **1,114** CITATIONS
SEE PROFILE

All in-text references underlined in blue are linked to publications on ResearchGate, letting you access and read them immediately.

Available from: Alessandro Pecora
Retrieved on: 16 January 2016

Sensors and Actuators B 155 (2011) 768–774

Contents lists available at ScienceDirect

Sensors and Actuators B: Chemical

journal homepage: www.elsevier.com/locate/snb

Flexible sensorial system based on capacitive chemical sensors integrated with readout circuits fully fabricated on ultra thin substrate

E. Zampetti*, L. Maiolo, A. Pecora, F. Maita, S. Pantalei, A. Minotti, A. Valletta, M. Cuscunà, A. Macagnano, G. Fortunato, A. Bearzotti.

Consiglio Nazionale delle Ricerche – Istituto per la Microelettronica e Microsistemi (CNR–IMM), Via del Fosso del Cavaliere 100, 00133 Roma, Italy

ARTICLE INFO

Article history:
Received 22 October 2010
Received in revised form 19 January 2011
Accepted 24 January 2011
Available online 1 February 2011

Keywords:
Flexible sensor
Ultra thin substrate
Capacitive sensor
Flexible electronics
Alcohols

ABSTRACT

In this paper we present the design and fabrication of a fully flexible sensorial system, composed of three different sensor units implemented on an ultrathin polyimide substrate of 8 μm thick. Each unit is composed by a capacitive chemical sensor integrated with readout electronics. The sensors are parallel plate capacitors with the top electrode properly patterned to allow analytes diffusion into the dielectric that acts as chemical interactive material. Three different polymers, poly(tetrafluoroethene) (PTFE), poly(methyl 2-methylpropenoate) (PMMA) and benzocyclobutene (BCB), were used as dielectrics. A ring oscillator circuit, implemented with polysilicon thin film transistors (PS-nTFT), was used to convert the capacitance variations into frequency shifts. The electronic tests show oscillating frequencies of about 211 ± 2 kHz and negligible frequency shifts under different bending radius conditions. Furthermore, system response to some alcohols concentrations (Methanol, ethanol, 1-butanol, and 1-propanol) is reported and data analysis proves that the system is able to discriminate methanol from ethanol.

© 2011 Elsevier B.V. All rights reserved.

1. Introduction

Nowadays, the world sensors market is in continuous growing thanks to several new applications that can improve products in different areas like automotive manufacturing, biomedical industry and consumer electronics (it was about 30 billion of dollars in the 1998 and about 50 billion of dollars in the 2008) [1]. In particular, chemical sensors find applications in many fields, as in the detection of single gases (CO_2, CO, CH_4, etc.), volatile organic compounds (VOC) as alcohols, hydrocarbons, amines or smells generated from food or household products [2,3].

Multisensor systems or electronic nose are the modern gas sensing devices designed to analyze such complex analytes mixtures [4–6]. In the last years new challenges have emerged in sensor market, in particular a growing demand for chemical sensors adaptable to non planar surfaces, weightless, inexpensive and with integrated front-end electronics. For this reason, new low temperature fabrication technologies such as printed electronics or system on foil electronics are deeply investigated for the development of new materials and manufacturing processes compatible with flexible polymeric substrates [7]. The tagging of the alimentary products, directly on the food or on its package, or the monitoring of human health directly on the skin of patients, are two examples of new applications where flexible sensors could be successfully exploited [8–10].

In this work we show the design, fabrication and test of a fully flexible sensorial system (SS), composed of three different sensor units (SU), integrated on an ultrathin polyimide substrate (PI) of 8 μm thick. Each SU consists of a capacitive sensor connected to an ring oscillator (RO) used as readout circuit. In each unit we utilized a different chemical interactive material (CIM) as dielectric polymer: poly(tetrafluoroethene) (PTFE), poly(methyl 2-methylpropenoate) (PMMA) and benzocyclobutene (BCB). These materials can be easily handled since they are commonly used in microelectronic process as passivation layer or photoresist. These characteristics make possible a large scale production.

Each CIM is able to detect diverse analytes depending from the diffusion capability of the particular gas into the dielectric matrix [11–13]. In fact, once the analyte is absorbed into the sensor, a combination of different mechanisms can take place. These phenomena change the capacitance relative dielectric constant because of structure modification and/or polymer swelling obtaining a specific sensor sensitivity to that analyte [14].

Two main strategies are generally adopted to develop this kind of sensor: the first uses thick planar interdigitated metal electrodes covered by a CIM; the second uses a CIM between two metal electrode layers, where the top layer is patterned to allow the interaction with analytes. As reported in several papers, the feasibility and the efficiency of both methods to develop flexible capacitive sensors have been demonstrated [15–18]. The second

* Corresponding author. Tel.: +39 06 49934572; fax: +39 06 49934066.
E-mail address: emiliano.zampetti@artov.imm.cnr.it (E. Zampetti).

0925-4005/$ – see front matter © 2011 Elsevier B.V. All rights reserved.
doi:10.1016/j.snb.2011.01.045

strategy, unlike the first [19–23], allows to use thick layer of CIM with thin layers of metal electrodes without altering system flexibility and sensor functioning, as reported in our previous paper [24]. For these reasons, we adopted this strategy to develop the SS, fabricating the capacitive flexible sensor with two metal layers (top and bottom), where the top electrode is patterned in squares in order to allow the analytes diffusion into the CIM.

To demonstrate the feasibility of the proposed fully flexible capacitive platform and to evaluate the system response, some electronic measurements have been performed in presence of four different VOCs. In particular, electronic tests proved the correct functioning of the RO and the dependence of the frequency shift from the variation of the sensor capacitance. Furthermore, principal component analysis (PCA) [25] has been calculated showing that, the SS allows the discrimination of methanol from ethanol. This result could be of a certain interest in food applications [26] and encourage the further developing of the sensorial systems based on capacitive flexible sensor technology.

2. System design

The proposed SS was composed of three different sensor units (SU), reaching a final dimension of about 10 mm × 3 mm. Each SU was processed on a single wafer separately and then peeled off from the rigid carrier and fixed together on a common freestanding PI film, reaching an overall thickness of about 35 μm. With this approach we avoided issues related to chemical compatibility among different CIMs, reducing the complexity of the whole fabrication process.

In this work BCB, PTFE and PMMA have been used as CIM. Frequency changes of the three output signals (F_{OUTi}) are related to the capacitive variations and then to the concentration of the adsorbed analytes in the different dielectric polymers. The SS proposed maintains an high integration level allowing a properly signal processing that facilitates data reading and decreases noise to signal ratio.

2.1. Sensors units design

As previous described, each SU was composed of a capacitive sensor with an integrated ring oscillator based on Low Temperature Poly-Silicon process (LTPS) developed on PI substrate [27]. The capacitive sensor consists of three layer structure (as a sandwich), bottom metal electrode (A), top metal electrode (B) and dielectric material (CIM), fabricated over an insulating substrate of PI (Fig. 1).

Sensor layout has been designed to optimize the performances in terms of response time and electric field coupling, aided by 3D finite element simulations. To allow the analytes diffusion into the

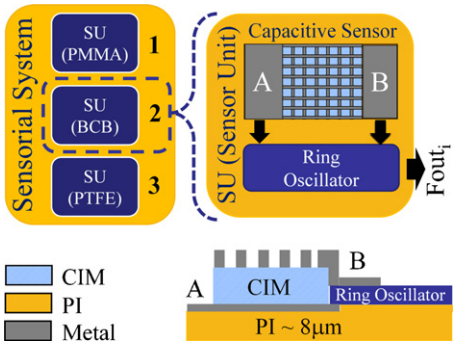

Fig. 1. Scheme of the Sensorial System (SS) comprising three different sensor units (SU) fixed on a free standing foil of PI. Each SU consists of a capacitive sensor and a ring oscillator circuit. (A and B) were the bottom and the top electrodes respectively. The top electrode was patterned to allow the analyte permeation through the CIM. F_{OUTi} (i: 1, 2, 3) were the SS output signals.

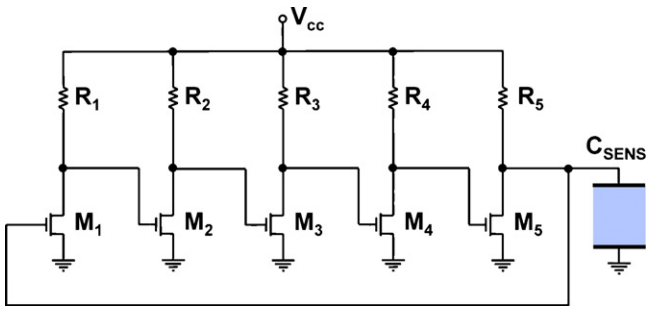

Fig. 2. Schematic view of a five stages ring oscillator circuit (RO) integrated to a capacitive sensor on flexible PI substrate. M_i and R_i (with i; 1, 2, 3, 4, 5) were the PS-nTFTs and polysilicon load resistors respectively, that implement the inverter gates, while the capacitor C_{SENS} represents the sensor capacitance.

dielectric material, top electrode must be shaped with some openings: in particular, the simulations have shown that the square pattern for the top electrode is the best choice, as well described in our previous works [24]. The top electrode of the capacitor has been chosen with an area of about 1.5 mm × 1.5 mm and a transparency factor of 50%. This device shape has been taken to match the sensor capacitance value with the interface circuit characteristics (e.g. maximum load capacitance value, oscillating frequency and parasitic capacitance values).

Several circuit configurations can be adopted in order to interface a capacitive sensor using different conversion techniques or strategies: switched capacitors, sigma-delta converter, amplitude modulation technique, oscillation circuits, etc.[28–33]. We selected the simplest circuit interface based on RO made by low temperature n-channel polysilicon thin film Transistor (PS-nTFT) directly integrated on PI [34–36]. The RO circuit [37] consists of a cascade of five identical inverter gates, as depicted in Fig. 2. The output of the fifth inverter was connected to the input of the first one. Since the circuit has only one stable operating point in DC mode (the logic inverter threshold voltage), it is inherently unstable. In this way, when any of the gate input or output voltage diverges from the unstable operating point the circuit starts to oscillate. In first approximation, the period τ_{OUT} of the oscillating signal is given by

$$\tau_{OUT} = (N-1)\cdot\tau_{INV} + \tau_{SENS} \quad (1)$$

where N is the number of the stages, τ_{INV} is the propagation delay time of a single inverter (depending on the load resistor value, the parasitic capacitances and the PS-nTFT dynamic parameters), while τ_{SENS} is the delay time of the last stage, affected by sensor capacitance value C_{SENS}. According to the Eq. (1), the ring oscillator circuit converts the sensor capacitance variations into the oscillation frequency shift F_{OUT} as shown in Eq. (2).

$$F_{OUT} = \frac{1}{\tau_{OUT}} \quad (2)$$

In order to properly design integrated readout interface, circuit simulations have been performed with the AIM-Spice software. The model used for PS-nTFT simulations is a semi-empirical, physical based analytical model (RPI) [38,39]. It can be used for all modes of DC operation (leakage, sub-threshold, above threshold and kink regime) and it includes a capacitance model for simulation of dynamic operation, taking into account also temperature effects. In the proposed RO each stage is a simple PS-nTFT (M_i) loaded by a n-poly resistor (R_i), see in Fig. 2. The dimensions of M_i are W = 150 μm, L = 10 μm and R_i = 200 kΩ with i = 1, 2, 3, 4, and 5. The allowed supply voltages V_{CC} can vary from 8 to 15 V. Simulation results have shown that oscillating frequency, for a five stage RO and for a C_{SENS} = 50 pF, is about 220 kHz.

Table 1
Sensor capacitance values obtained after the process optimization and measured at room temperature in nitrogen atmosphere.

Polymer	Capacitance (pF)
BCB	50 ± 4 pF
PTFE	49 ± 5 pF
PMMA	53 ± 3 pF

3. Experimental

Each SU is realized according to a non self-aligned polysilicon PS-nTFT technology already shown in previous work [24]. This fabrication process allows to integrate on the same ultra thin flexible substrate both the capacitive sensors and the RO circuit. It is based on temporary bonding technique between the flexible substrate and a conventional Si-wafer. This gives the possibility of using a standard semiconductor equipment overcoming problems of handling freestanding plastic sheets and plastic shrinkage at high temperature processing.

As first fabrication step we spin a polyimide precursor layer on 3″ thermally oxidized Si wafer. The polyimide is then placed in oven and cured at the maximum temperature of 350 °C in nitrogen atmosphere. This drives off solvents as well as initiates the imidization reactions that gives to the final polyimide film its desirable properties. With this procedure, we obtain a polyimide layer of about 8–10 μm thick. Then we grow a buffer layer composed of silicon nitride and silicon dioxide respectively of 50 nm and 400 nm thick followed by an amorphous silicon film of 70 nm thick, using a low temperature plasma – enhanced chemical vapor deposition (PECVD) technique (<350 °C). Source and drain contacts and circuit resistances are lithographically patterned after the deposition of a phosphorous doped silicon layer of 20 nm. The active a-Si layer is then dehydrogenated and poly-crystallized combining a low temperature annealing technique (300 °C) with an excimer laser irradiation. At this step the n-doped regions are simultaneously activated. Each circuit element is then isolated removing the active material in reactive ion etching (RIE) and a gate dielectric layer is deposited at room temperature by electron cyclotron resonance plasma-enhanced chemical vapor deposition (ECR-PECVD). Via-holes are patterned and aluminum is thermally evaporated realizing, at the same time, PS-nTFTs source, drain and gate contacts, metal circuit connections and the bottom metal electrode (A) of the capacitive sensors (Fig. 1). At this step several kind of CIMs (dielectric materials for the capacitors) can be deposited, depending by the specific SU and the fabrication is completed by depositing and patterning the upper metal layer. Finally, to test the three sensor units in the same conditions, each SU was peeled off from the rigid silicon wafer and then fixed and connected to another free standing foil of PI.

In particular, in this work we have developed and tested three types of SUs based on three different polymers: the first one was fabricated with 850 nm of BCB by Dow Chemical Company, spin coated and dried in furnace at a temperature of 250 °C for 1 h. The second was realized with a PTFE-like film of about 500 nm deposited by using a 50% CHF_3/Ar gas mixture in a reactive ion etching reactor (RIE) at a working pressure of 300 m Torr for 45 min [40]. The last one, was based on 650 nm of PMMA (ARP-639 e-beam resist PMMA 50K by Allresist) spin coated and dried at 170 °C for 5 min. In order to optimize the fabrication process of the SUs, a set of 30 capacitive sensors based on the same polymer, without readout circuit have been fabricated and tested separately. Table 1, shows the sensor capacitance values, obtained for the three different polymers at the end of optimization process.

In the same way, to test the circuit performances (oscillating frequency, signal amplitudes, frequency shifts versus capacitance changes, parasitic capacitances, etc.) some separated batches of this circuit, without sensor, were fabricated. In Fig. 3, a ring oscillator on PI with five stages is shown. Each stage was realized by a PS-nTFTs ($M_{1\ldots5}$) connected to a common ground pad and loaded by a n-poly resistor (R_i,) with a meander structure to implement the inverter gate.

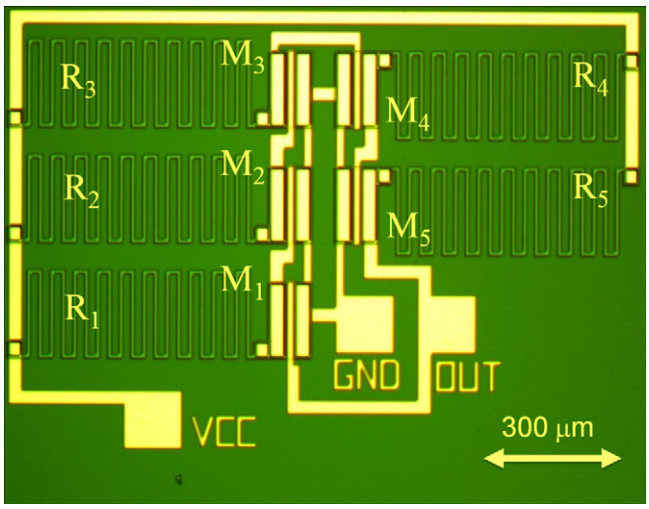

Fig. 3. Optical image of a five stages RO fabricated on flexible PI (8 μm) separately from the sensor. The V_{CC}, GND and OUT pads were used to test the circuit by means of an electronic probe station. The dimensions of PS-nTFT were: W = 150 μm, L = 10 μm.

At the end of the optimization phase, we obtained all the design rules to create the SUs for the fabrication of the SS. In Fig. 4a and b is shown a sample of PI foil, before and during the peeling from the rigid carrier (silicon wafer). The sample consisted of approximately 400 units of sensors based on the same CIM, also the SUs (about 3 mm × 2 mm) were spaced to allow the cutting process. A detail of SU layout after the fabrication is reported in Fig. 4c, where it is possible to see both a portion of the patterned top electrode (b) of the capacitive sensor and the ring oscillator circuit, on the right.

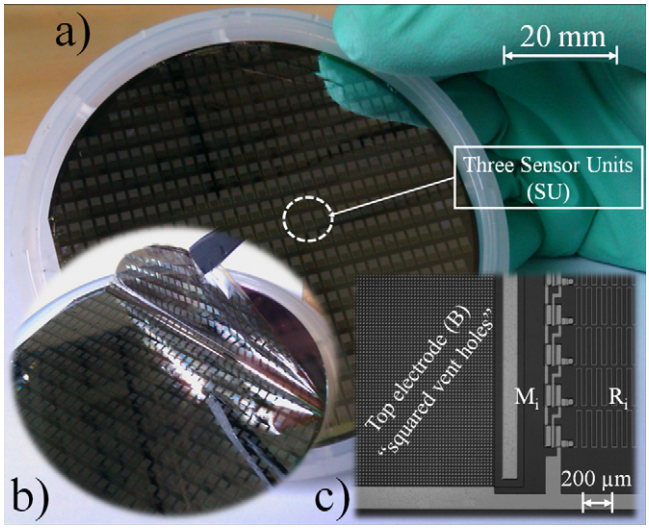

Fig. 4. A example of a fabricated sensor unit. (a) 3″ PI substrate comprising about 400 SUs before the peeling from the rigid carrier, (b) semi-transparent, very bendable foil of PI about 10 μm thick during the peeling process, and (c) optical image showing both a portion of the capacitive sensor (on the left) and the ring oscillator circuit (on the right). The overall dimensions of SU was about 3 mm × 2 mm.

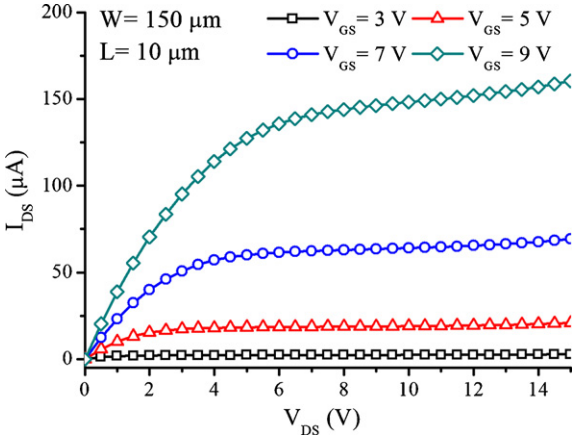

Fig. 5. An example of the measured output characteristics (I_{DS} vs. V_{DS}) of a fabricated PS-nTFT where $\mu_e \sim 60\,cm^2/V\,s$, $V_T \sim 4, 5$, $W = 150\,\mu m$ and $L = 10\,\mu m$.

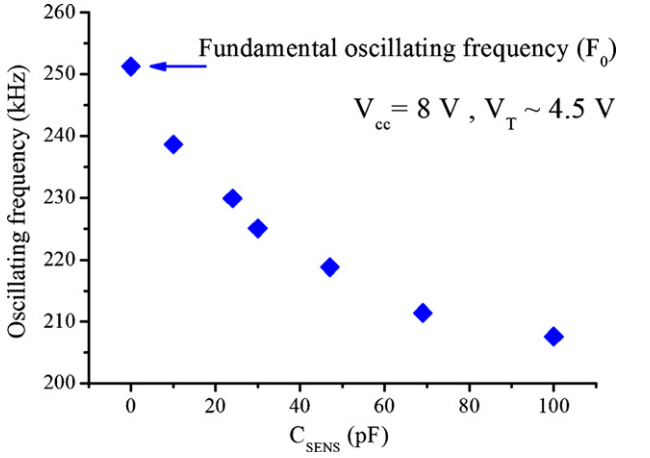

Fig. 7. Frequency shift caused by the insertion of an external capacitor (C_{SENS}), the capacitance was varied, from 0 to 100 pF, F_0 is the oscillating frequency when $C_{SENS} = 0$.

4. Results and discussion

4.1. Ring oscillator circuits test

As described above the ring oscillator circuit, fabricated without capacitive sensor, has been tested focusing on two different features: DC measurements of a single PS-nTFT in order to extract electrical and physical parameters (e.g. electronic mobility, threshold voltage, ohmic resistance for low V_{DS}, saturation properties and electrical stability) and dynamic analysis (e.g. output signal amplitude, oscillating frequency, frequency shifts versus sensor capacitance changes, etc...). In Fig. 5 the output characteristics (I_{DS} vs. V_{DS}) of a fabricated PS-nTFT ($W = 150\,\mu m$ and $L = 10\,\mu m$) for a variable gate-source voltage V_{GS} are shown. From DC measurements performed on different samples of PS-nTFT we have calculated a mobility (μ_e) of $\sim 60\,cm^2/V\,s$ and a threshold voltage (V_T) of $\sim 4.5\,V$.

In order to evaluate the correct functioning of the RO both in absence and in presence of the capacitive sensor, we have connected (by external probes) to the output of RO some capacitors (test load capacitors) realized with the same polymers and fabrication method of the capacitive sensors. In Fig. 6 is reported an example of the trend of the output signal V_{OUT} with (C_{SENS}: 15, 25 pF) and without load capacitor ($C_{SENS} = 0$ pF) and with a $V_{CC} = 8\,V$. Several RO circuits have been measured and we have observed that in the case of $V_{CC} = 8\,V$, $V_T \sim 4.5\,V$ and $C_{SENS} = 0$ pF, the V_{OUT} shown an oscillating frequency, $F_{OUT} \sim 250\,kHz \pm 15\,kHz$ and a peak-to-peak amplitude $V_{pp} \sim 3\,V \pm 0.8\,V$. It is well known that the frequency value depends from the parasitic elements (capacitors, resistors, etc.) both of the PS-nTFTs and of the circuit layout.As shown in Fig. 6, when the value of C_{SENS} increases, the amplitude of the signal V_{OUT} decreases up to stop the oscillation of the circuit for very large values of C_{SENS}. This phenomenon may be related to increases in load current, but it is negligible when the capacity changes (ΔC_{SENS}) are very small and about the value of 50 pF. In fact, this value was used as a design value for capacitive sensors and we believe this problem could be solved, even for large variations of C_{SENS}, connecting to the output signal an another inverter, operating as buffer. The trend of F_{OUT} in presence of different load capacitors, $C_{SENS} = 0$, 10, 24, 30, 47, 69, 100 pF, is reported in Fig. 7.

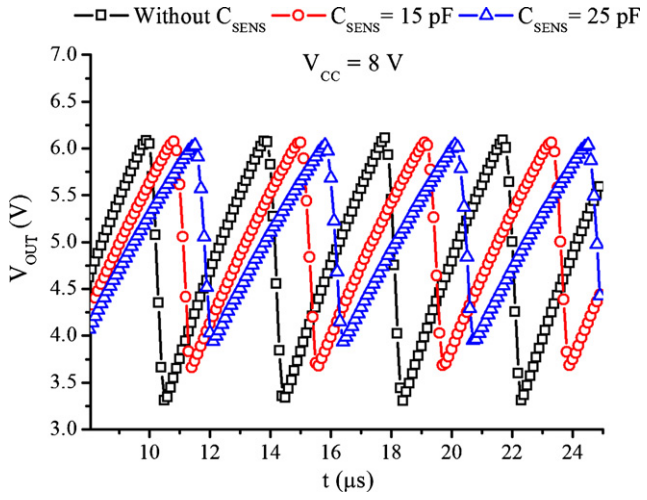

Fig. 6. Measured RO output signal V_{OUT} in loaded ($C_{SENS} = 15$, 25 pF) and unloaded ($C_{SENS} = 0$) conditions with $V_{CC} = 8\,V$ and $V_T \sim 4.5\,V$. The average values, for the amplitude and the oscillating frequency were $F_{OUT} \sim 250\,kHz \pm 15\,kHz$ and $V_{PP} \sim 3\,V \pm 0.8\,V$, in the unloaded case $C_{SENS} = 0$.

The measured frequency showed a stability of about ±5–8 Hz (not shown in Fig. 7) around the fundamental oscillating frequency value: this feature produces negligible errors in the circuit functioning (capacitance changes into frequency shifts).

The ideal output signal of a standard ring oscillator circuit can be represented by a rectangular wave [37]. This behavior shows such shape when each inverter composing RO has same characteristics, in terms of rise time, fall time and threshold voltage, of the devices that implement the inverter gates (e.g. CMOS). On the contrary, the output signal of our circuit, is similar to saw-tooth wave: this typical shape is caused by slightly different features of single inverter gate and by the presence of passive loads (R_i) that produce different rise time and fall time. However, the circuit functioning is not compromised and it can be successfully utilized as readout circuit for our purpose.

4.2. System performances under VOC concentrations

As previous described, each different SU has been realized in three separate substrates in order to simplify the entire fabrication process overcoming problems related to handling different CIM on the same device. At the end of the fabrication process, we have cut three SUs (one for each CIM type) and we have fixed them on a free standing PI substrate of 8 um. An anisotropic conductive tape (9703 by 3 M, of about 20 μm thin) has been used to fix the SUs onto the substrate and to create a good electrical contacts between the free standing substrate pads (V_{CC}, GND and the three F_{OUT}) and the electric contacts of the SUs. Once completed the entire

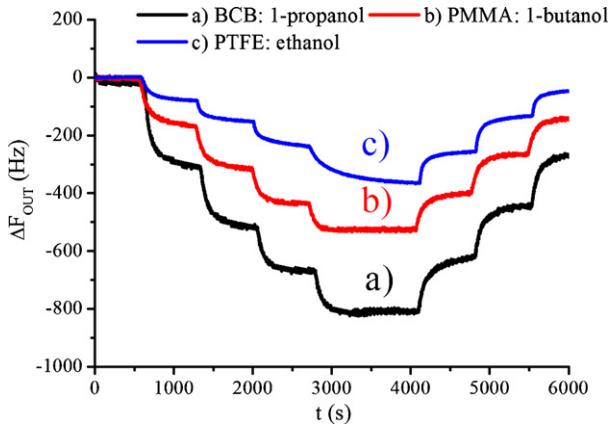

Fig. 8. An example of the dynamic responses of the BCB, PMMA and PTFE based SUs, reporting the frequency shifts (ΔF_{OUT}) towards pressure variations of alcohols reaching 6240 Pa for ethanol, 563 Pa for 1-butanol, 1848 Pa for 1-propanol.

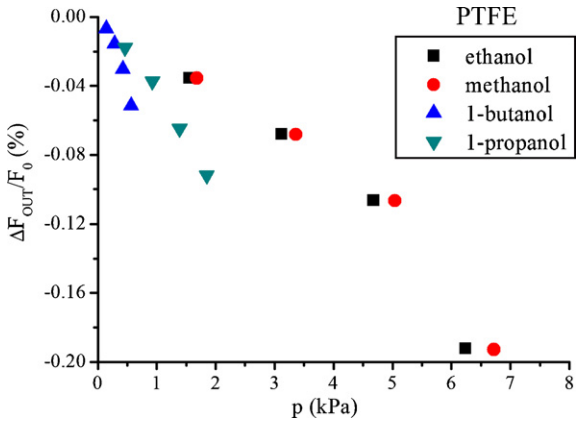

Fig. 9. Responses of the PTFE based SU, in terms of relative frequency shifts ($\Delta F_{OUT} \times 100/F_0$), versus increasing analyte partial vapor pressures.

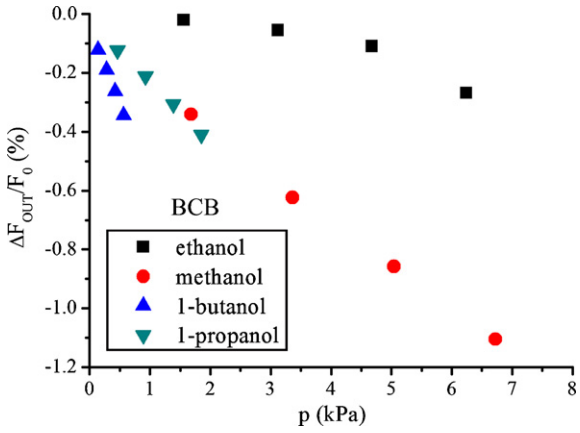

Fig. 10. Responses of the BCB based SU, in terms of relative frequency shifts ($\Delta F_{OUT} \times 100/F_0$), versus increasing analyte partial vapor pressures.

fabrication process the SS was placed in a test chamber analyzing sensor behavior to different VOCs. As already reported [41,42] the three polymers used in this work, show a significant sensitivity to the relative humidity concentrations and for this reason, in real world applications, a flexible humidity trap or a suitable encapsulation could be implemented, as reported in [43,44], to decrease its interference with VOC detections.

Several measurements have been performed with the purpose of investigate capacitive sensors stability. In particular, the SUs were tested for several hours under a relative humidity value of RH = 45% in order to evaluate the frequency drift due to the capacitance changes, when a DC supply was applied (data not shown). Although at the end of these experiments, we have observed a negligible frequency shift (up to 22 Hz), a dual power supply could be used to prevent the probability of ionic movement in the dielectric or ion accumulation on its surface. At a temperature of 22 °C and in nitrogen atmosphere, the sensors showed a capacitance value of 50 pF ($C_{SENS} = C_0$) for BCB, 49 pF for PTFE and 53 pF for PMMA. Moreover, to evaluate the system performances towards VOCs, we have analyzed the SUs responses versus partial pressure (p) variations of ethanol, methanol, 1-propanol, and 1-butanol. The variations of the analyte concentration were obtained by mixing two fluxes at different ratio: a dry flux of nitrogen and a flux of nitrogen loaded with the analytes, by means of a bubbler. The fluxes were controlled and supplied into measure chamber by a mass flow controller (MKS 147B), the total flux was maintained constant at 200 sccm. The partial vapor pressure of each component has been calculated by the Antoine equation at 22 °C [45], obtaining the following values: ethanol 6538 Pa, methanol 14,351 Pa, 1-propanol 2310 Pa and 1-butanol 704 Pa.

Fig. 8 shows an example of the dynamic responses of the SUs, reporting the frequency shifts $\Delta F_{OUT} = F - F_0$ towards partial pressure variations of three alcohols, where F_0 was the oscillating frequency, of each SUs, measured in presence of nitrogen.

The measures were performed varying the VOCs partial pressure each 700 s and reaching 6240 Pa for ethanol, 563 Pa for 1-butanol, 1848 Pa for 1-propanol as maximum values. The characteristics showed similar behaviors, in terms of response times and trend, both in the adsorption and in the desorption processes. The overall performances, in terms of percentage of relative frequency shifts ($\Delta F_{OUT} \times 100/F_0$) calculated at different alcohols vapor pressures are shown in Figs. 9–11.

These measures point out a specific behavior of each SU respect to the four alcohols examined. In fact, while the PTFE response is not able to discriminate between ethanol and methanol, it reveals different sensitivities (calculated as slope of the response curves) towards 1-butanol and 1-propanol. Moreover, PMMA and BCB SUs exhibit higher relative frequency spreads and a non linear behavior. For a single SU the sensitivity towards methanol and ethanol, calculated as the ratio between the percentage of relative frequency variation and analyte concentration expressed in parts per million (ppm) was, in the case of PMMA, 1.97×10^{-5}%/ppm and 7.78×10^{-6}%/ppm respectively. Considering that, the noise of this device was 4.8×10^{-3}%, the limits of detection are ~240 ppm and ~620 ppm. The sensitivity values are an order of magnitude lower

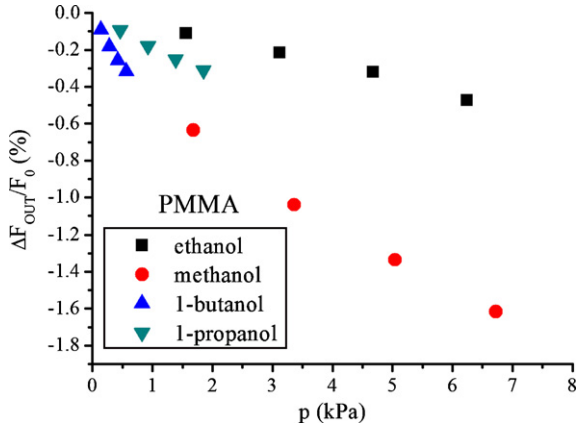

Fig. 11. Responses of the PMMA based SU, in terms of relative frequency shifts ($\Delta F_{OUT} \times 100/F_0$), versus increasing analyte partial vapor pressures.

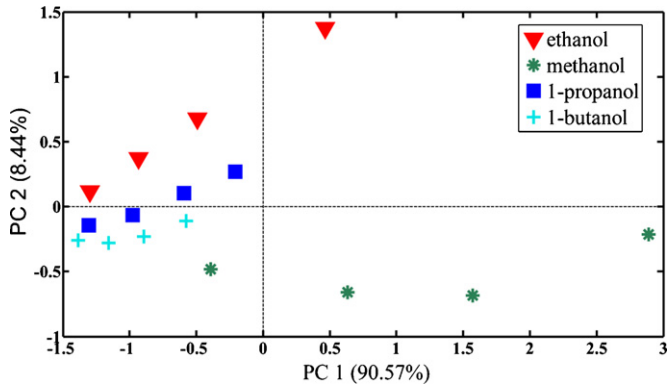

Fig. 12. Scores plot of the first two principal components (PC1, PC2).

than a not flexible sensorial system and comparable with a flexible sensor system as reported in literature [18,26].

All data concerning the SS responses towards VOCs were analyzed using standard multivariate data analysis techniques [46–48], by means of MATLAB 7.1 (The MathWorks Inc.) and PLS ToolBox 5.8 (Eigenvector Research Inc.).

An unsupervised classification analysis has been performed by using principal component analysis (PCA), in order to further identify how sensors can discriminate the different chemical compounds. The PCA was performed considering the 3-dimensional space of the sensor array responses to the different concentrations of ethanol, methanol, 1-propanol and 1-butanol. The relative frequency shift ($\Delta F_{OUT}/F_0$) was used in the feature extraction process to compose the data set. The scores plot of the first two principal components (PC1, PC2) is depicted in Fig. 12.

While different concentrations of methanol and ethanol showed their maximum variation on the PC1, the PC2 distinguished the concentrations of ethanol from methanol. From Fig. 12, it is possible to observe that the increasing concentrations, for each analyte, are distributed over vectors departing from the point where no chemical is delivered to the SS. In the space of two principal components (PC1, PC2) the responses to 1-butanol and 1-propanol are comprised between the responses to the ethanol and methanol. Fig. 13 shows the scores plot of the first two principal components after the data normalization performed to remove the concentration contribution. The normalization was implemented using Eq. (3) for each sensor response.

$$\overset{\text{norm}}{\Delta F_{OUT,i}} = \frac{\Delta F_{OUT,i}}{\sum_i \Delta F_{OUT,i}} \quad (3)$$

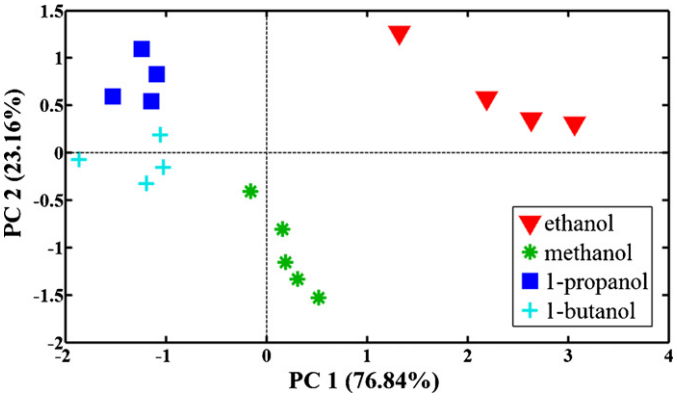

Fig. 13. Scores plot of the first two principal components (PC1, PC2) after the dataset normalization.

where *i* represents the different SUs. These preliminary results have showed that, the three SUs allow the discrimination of methanol from ethanol.

5. Conclusions

A flexible sensorial system composed by three sensor units, based on PTFE, PMMA and BCB polymers used as CIM, was designed, fabricated and tested. Sensor unit, consisting of a capacitive sensor interfaced with a ring oscillator circuit, was built on a thin flexible polyimide substrate using a low-temperature polysilicon Thin Film Transistors process. The electronic tests have shown oscillating frequencies of about 211 ± 2 kHz and negligible frequency shifts under bending conditions. System responses to several alcohols concentrations (Methanol, ethanol, 1-butanol, and 1-propanol) have emphasized a peculiar behavior of the sensor units versus tested analytes. These specific responses could be attributed to the different diffusion process and to the chemical affinity of the CIMs. Moreover also PCA analysis has confirmed the SS capability to discriminate methanol from ethanol. These preliminary results could pave a new way for large area flexible sensor applications.

References

[1] Press release by INTECHNO CONSULTING, Steinenbachgaesslein 49, CH-4051 Basel, Switzerland, http://www.intechnoconsulting.com.
[2] S. Ampuero, J.O. Bosset, The electronic nose applied to dairy products: a review, Sens. Actuators B 94 (2003) 1–12.
[3] J.W. Gardner, P.N. Bartlett, Electronic noses—Principles and Applications, Oxford University Press, 1999.
[4] F. De Cesare, S. Pantalei, E.A. Macagnano, Electronic nose and SPME techniques to monitor phenanthrene biodegradation in soil, Sens. Actuators B 131 (2008) 63–70.
[5] H. Yu, J. Wang, Discrimination of long Jing green-tea grade by electronic nose, Sens. Actuators B 122 (2007) 134–140.
[6] J.S. Vestergaard, M. Martens, P. Turkki, Application of an electronic nose system for prediction of sensory quality changes of a meat product (pizza topping) during storage, LWT – Food Sci. Technol. 40 (2007) 1095–1101.
[7] I. French, D. George, T. Kretz, F. Templier, H. Lifka, Flexible displays and electronics made in AM-LCD facilities by the EPLaR process, SID-Symposium Digest of Technical Papers 38 (May (1)) (2007) 1680–1683.
[8] H. Kudo, T. Sawada, M.X. Chu, T. Saito, H. Saito, K. Otsuka, Y. Iwasaki, K. Mitsubayashi, Flexible Glucose Sensor Using Biocompatible Polymers Sensors (2007) 620–623, 2006 5th IEEE Conference.
[9] F. Axisa, P.M. Schmitt, C. Gehin, G. Delhomme, E. McAdams, A. Dittmar, Flexible Technologies and Smart Clothing for Citizen Medicine, Home Healthcare, and Disease Prevention, IEEE Trans Inf Technol Biomed 9 (2005).
[10] E. Abad, S. Zampolli, S. Marco, A. Scorzoni, B. Mazzolai, A. Juarros, D. Gómez, I. Elmi, G.C. Cardinali, J.M. Gómez, F. Palacio, M. Cicioni, A. Mondini, T. Becker, I. Sayhan, Flexible tag microlab development: gas sensors integration in RFID flexible tags for food logistic, Sens. Actuators B 127 (2007) 2–7.
[11] T.E. Mlsna, S. Cemalovic, M. Warburton, S.T. Hobson, D.A. Mlsna, S.V. Patel, Chemicapacitive microsensors for chemical warfare agent and toxic industrial chemical detection, Sens. Actuators B 116 (2006) 192–201.
[12] P.L. Kebabian, A. Freedman, Fluoropolymer-based capacitive carbon dioxide sensor, Meas. Sci. Technol. 17 (2006) 703.
[13] C. Hagleitner, A. Hierlemann, D. Lange, A. Kummer, N. Kerness, O. Brand, H. Baltes, Smart single-chip gas sensor microsystem, Nature 414 (2001) 293–296.
[14] S.V. Patel, T.E. Mlsna, B. Fruhberger, E. Klaassen, S. Cemalovic, D.R. Baselt, Chemicapacitive microsensors for volatile organic compound detection, Sens. Actuators B 96 (2003) 541–553.
[15] A. Oprea, J. Courbat, N. Bârsan, D. Briand, N.F. deRooij, U. Weimar, Temperature humidity and gas sensors integrated on plastic foil for low power applications, Sens. Actuators B 140 (2009) 227–232.
[16] C. Wang, K. Huang, D. Lin, W. Liao, H. Lin, Y. Hu, A flexible proximity sensor fully fabricated by inkjet printing, Sensors 10 (2010) 5054–5062.
[17] A. Arena, N. Donato, G. Saitta, Capacitive humidity sensors based on MWCNTs/polyelectrolyte interfaces deposited on flexible substrates, Microelectron. J. 406 (2009) 887–890.
[18] S.J. Kim, Flexible alcohol vapor sensors using multiple spray-coated SWNTs on PES substrates, J. Korean Phys. Soc. 54 (2009) 1779-1783 (5 PART 1).
[19] C.J. Dias, Dielectric response of interdigital chemocapacitors: The role of the sensitive layer thickness, Sens. Actuators B 115 (2006) 69–78.
[20] C. Laville, C. Pellet, Comparison of three humidity sensors for a pulmonary function diagnosis microsystem, IEEE Sens. J. 2 (2002).
[21] Z. Suo, E.Y. Ma, H. Gleskova, S. Wagner, Mechanics of rollable and foldable film-on-foil electronics, Appl. Phys. Lett. 74 (1999).
[22] S. Wagner, S.J. Fonash, T.N. Jackson, J.C. Sturm, Proc. SPIE 4362 (2001) 226–244.

[23] H. Gleskova, S. Wagner, W. Soboyejo, Z. Suo, Electrical response of amorphous silicon thin-film transistors under mechanical strain, J. Appl. Phys. 92 (2002).
[24] E. Zampetti, S. Pantalei, A. Pecora, A. Valletta, L. Maiolo, A. Minotti, A. Macagnano, G. Fortunato, A. Bearzotti, Design and optimization of an ultra thin flexible capacitive humidity sensor, Sens. Actuators B 143 (2009) 302–307.
[25] I.T. Jolliffe, Principal Component Analysis, Springer, 2002.
[26] C. Wongchoosuk, A. Wisitsoraat, A. Tuantranont, T. Kerdcharoen, Portable electronic nose based on carbon nanotube-SnO_2 gas sensors and its application for detection of methanol contamination in whiskeys, Sens. Actuators B 147 (2010) 392–399.
[27] A. Pecora, L. Maiolo, M. Cuscunà, D. Simeone, A. Minotti, L. Mariucci, G. Fortunato, Low-temperature polysilicon thin film transistors on polyimide substrates for electronics on plastic, Solid State Electron. 52 (2008) 348–352.
[28] U. Schoeneberg, B.J. Hosticka, G. Zimmer, G.J. Maclay, A novel readout technique for capacitive gas sensors, Sens. Actuators B 1 (1990) 58–61.
[29] A. Gaisser, W. Geiger, T. Link, J. Merz, S. Steigmajer, A. Hauser, H. Sandmaier, W. Lang, N. Niklasch, New digital readout electronics for capacitive sensors by the example of micromachined gyroscopes, Sens. Actuators A 97 (2002) 557–562.
[30] Z. Ignjatovic, M.F Bocko, An interface circuit for measuring capacitance changes based upon capacitance-to-duty cycle (CDC) converter, IEEE Sens. J. 5 (2005) 403–410.
[31] B. Wang, T. Kajita, T. Sun, C. Temes, High-accuracy circuits for on-chip capacitive ratio testing and sensor readout, IEEE Trans. Instrum. Meas. 47 (1998) 16–20.
[32] C.Y. Hsieh, C.S. Chen, W. A: Tsou, et al., A flexible mixed-signal/RF CMOS technology for implantable electronics applications, J. Micromechan. Microeng. 20 (2010).
[33] T. Afentakis, M. Hatalis, A.T. Voutsas, et al., Design and fabrication of high performance polycrystalline silicon thin-film transistor circuits on flexible steel foils, IEEE Trans. Electron Dev. 53 (2006) 815–822.
[34] C.L. Dai, A capacitive humidity sensor integrated with micro heater and ring oscillator circuit fabricated by CMOS-MEMS technique, Sens. Actuators B 122 (2007) 375–380.
[35] S. Park, C. Min, S. Cho, A 95nW ring oscillator-based temperature sensor for RFID Tags in 0.13 mu m CMOS, ISCAS IEEE International Symposium On Circuits And Systems 1–5 (2009) 1153–1156.
[36] C.L. Dai, P.W. Lu, C.L. Chang, C.Y. Liu, Capacitive micro pressure sensor integrated with a ring oscillator circuit on chip, Sensors 9 (2009) 10158–10170.
[37] S.M. Kang, Y. Leblebici, Digital Integrated Circuits, McGraw-Hill, New York, 1996.
[38] M.D. Jacunski, M.S. Shur, A.A. Owusu, T. Ytterdal, M. Hack, B. Iñiguez, A short channel DC SPICE model for polysilicon thin film transistors including temperature effects, Ieee Trans. Electron. Dev. 46 (1999).
[39] M. Valdinoci, L. Colalongo, G. Baccarani, G. Fortunato, A. Pecora, I. Policicchio, Floating body effects in polysilicon thin film transistors, IEEE Trans. Electron. Dev. 44 (1997) 2234–2241.
[40] M. Rapisarda, D. Simeone, L. Mariucci, M. Cuscuna', L. Maiolo, A. Minotti, S. Pantalei, A. Pecora, A. Valletta, G. Fortunato, PTFE-like encapsulation layer for pentacene Thin Film Transistors ICOE09 – International Conference on Organic Electronics (2009).
[41] C. Laville, C. Pellet, Comparison of three humidity sensors for a pulmonary function diagnostic microsystems, IEEE Sens. J. 2 (2002) 96–101.
[42] Y. Sakai, Y. Sadaoka, M. Matsuguchi, Humidity sensors based on polymer thin films, Sens. Actuators B 35 (1996) 85–90.
[43] Kalfon, Rami Abraham (Kfar-Shmuel, IL), Flexible moisture-barrier packages and methods of producing same (2009) United States Patent 20,090,218,247.
[44] J. Courbat, D. Briand, N.F. de Rooij, Reversed processing of dry photoresist: application to the encapsulation of chemical sensors, Procedia Eng. 5 (2010) 335–338.
[45] NIST Chemistry WebBook, http://webbook.nist.gov.
[46] M.P. Marti, R. Boque, O. Busto, J. Guasch, Electronic noses in the quality control of alcoholic beverages, Trends Anal. Chem. 24 (2005) 57–66.
[47] S.N. Deming, Y. Michotte, D.L. Massart, L. Kaufman, B.G.M. Vandeginste, Chemometrics: A Textbook, Elsevier, 1988.
[48] I.T. Jolliffe, Principal Component Analysis, Springer (2002).

Biographies

Emiliano Zampetti received the Master degree in Electronics Engineering in 2002 and the Ph.D. on "Engineering Of sensorial and learning systems" in 2007 from "Università degli studi di Roma Tor Vergata". Currently he works as researcher (non-permanent position) at the Institute for Microelectronics and Microsystems of the National Research Council (CNR-IMM). His research interests are concerned with the design and development of the electronic circuits for Electronic Nose Systems, electronic readout circuits for gas sensor, electrospinning apparatus for nanotechnology applications and bio-electronic noise in cells and neurons.

Luca Maiolo received the Master degree in Physics in 2003 and the Ph.D. on "Realization and characterization of polysilicon based electronic devices on flexible substrates for electronics on plastic" in 2008, both from "Università degli studi di Roma Tre". Currently, he is a post-doctoral research assistant at the Institute for Microelectronics and Microsystems of the National Research Council (CNR-IMM). His research is mainly focused on fabrication and characterization of electronic circuits and smart sensors integrated on flexible substrates.

Alessandro Pecora was born in Rome, Italy, on 1962. He is researcher at the Institute for Microelectronics and Microsystems of the National Research Council in Rome. He received the Master degree in Physics from the "Università degli studi di Roma La Sapienza", in 1990. His present interest is focused on the development of Thin Film Transistors on flexible substrate. His main research fields are related to microelectronics process, excimer laser crystallization, devices and material characterizations.

Francesco Maita was born in Rome, Italy in 1984. He received Master degree in Electronics Engineering from "Università di Roma Tor Vergata" in 2009. Currently he is a Ph.D. student on "Engineering Of sensorial and learning systems" and his studies are focused on the development of electronics on flexible substrate.

Simone Pantalei received the Master degree in Electronics Engineering in 2002, and the Ph.D. on "Engineering Of sensorial and learning systems" in 2007 from "Università degli studi di Roma Tor Vergata". Currently he works as researcher (non-permanent position) at Institute for Microelectronics and Microsystems of the National Research Council (CNR-IMM). His research interest include the enhancement of the sensing capabilities of the Quartz Crystal Microbalances, design of Multichannel Quartz Crystal Microbalance, finite elements analysis applied to gas sensing systems.

Antonio Minotti is currently working at CNR-IMM in Rome as technician. He received first level degree in Material Science in 2002 from "Università degli studi di Roma Tre". His research activities have been focused mainly on MEMS systems, C-MUT (Capacitive Micromachined Ultrasonic Transducers) and recently on microfabrication processes and thin-film depositions on flexible substrates.

Antonio Valletta was born in Salerno, Italy, in 1971. He received the Master degree in Physics from the "Università di Roma La Sapienza" in 1997 and in the PhD degree in Physics in 2003 defending a thesis on the analysis and characterization of polycrystalline silicon PS-nTFTs. In November 2007, he moved from Solid State Electronic Institute to IMM Rome, where he works as researcher. His current research interests include the modeling, simulation and physics of polycrystalline silicon TFTs and organic, pentacene based, TFTs.

Massimo Cuscunà was born in Rome, in 1977. He received the Master degree and the Ph.D. degree in physics from the "Università degli studi di Roma Tre", in 2002 and 2005 respectively. From 2001 to 2007 he worked on polysilicon thin film transistor fabrication process on rigid carrier and several flexible substrates. Currently he works as researcher (non-permanent position) at Institute for Microelectronics and Microsystems of the National Research Council (CNR-IMM). His current research interests include silicon nanowire growth and characterization for gas sensor and photovoltaic application.

Antonella Macagnano is Research Scientist at the Institute of Microelectronics and Microsystems (IMM) of CNR (since 2001). She graduated in Biological Sciences at the University of Lecce, Lecce, Italy, in 1993 and obtained professional degree as Biologist, in 1994. Mainly, her research activities have concerned the study, the design, the characterization and the optimization of chemical (metallo-porphyrins, cavitands, metallo-oligomers and nanostructured polymers) and biological membranes (oligopeptydes, bio-polymers) for selective interactions with both gases and volatile organic compounds. She has been involved in several International and National research projects focused on design, improvement and implementation of sensor devices for environment, health and agri-food industry.

Guglielmo Fortunato is research director and is responsible of the "Devices for large area electronics" Unit at IMM-CNR. He has been a visiting scientist at the Tokyo Institute of Technology (1983) and at GEC-Hirst Research Center (1985–1986). His main scientific activity is on the physics and technology of inorganic (amorphous, micro- and polycrystalline silicon) and organic (pentacene) thin film transistors. Recently he focused on flexible electronics, application of excimer laser annealing for polysilicon PS-nTFTs and shallow junction formation. He has been responsible of several National (9) and European (6) Research contracts and also of industrial research contracts with ST-Microelectronics, Philips, THALES, GEC-Marconi. He was part-time professor of Semiconductor Device Physics at the Roma III University between 2001 and 2006. He has been co-organiser of several E-MRS Symposia and has been recently Chairman of the Third International Thin Film Transistor Conference (Rome, 24–25 Jan. 2007).

Andrea Bearzotti was born in Udine, Italy on 19 October 1960. He received the Italian Laurea degree in Physics from the "Università degli studi di Roma La Sapienza" in February 27, 1986 with a thesis titled "M.O.S. structure with palladium gate as hydrogen and oxygen sensor". He then joined the "Solid State Electronic Institute" of the C.N.R. on September 1, 1988 where he was working in the field of solid-state sensors. From February 1998 he's working at the Microelectronics and Microsystems Institute (I.M.M. – C.N.R.). His present interest is focused on the development of mesostructured materials for chemical sensors.